Journal of Statistics & Management Systems
ISSN 0972-0510 (Print), ISSN 2169-0014 (Online)
Vol. 27 (2024), No. 7, pp. 1473–1497
DOI : 10.47974/JSMS-1237

Secant Topp-Leone family of distributions : Properties, regression and applications

Salifu Nanga *
Department of Basic Sciences
School of Basic and Biomedical Science
University of Health and Allied Sciences
H0E
Ghana

Suleman Nasiru †
Department of Statistics and Actuarial Science
School of Mathematical Sciences
C. K. Tedam University of Technology and Applied Sciences
Navrongo BOL
Ghana

Jakperik Dioggban §
Department of Biometry
School of Mathematical Sciences
C. K. Tedam University of Technology and Applied Sciences
Navrongo BOL
Ghana

Abstract

The Secant Topp-Leone (STL) generator, which is developed by combining the TL and secant distribution families, is discussed in this paper. We address various statistical characteristics of this new family. We also present five special distributions within this family and demonstrate their flexibility. These distributions' parameters are estimated using the maximum likelihood estimation (MLE) technique, and Monte Carlo simulations are used to assess the estimation technique's accuracy. The choice of estimation method used in the study was validated by results from the Monte Carlo experiment's biases, RMSEs, average width, and coverage probability. Using two real datasets, the Secant Topp-Leone Burr III

* *E-mail:* **snanga@uhas.edu.gh;**
nanga.salifu@gmail.com (Corresponding Author)
† *E-mail:* **sulemanstat@gmail.com;**
snasiru@cktutas.edu.gh
§ *E-mail:* **jdioggban@gmail.com**

(STLBIII) distribution performs better than other well-known distributions. Additionally, the natural logarithm of secant Topp-Leone Burr XII (LSTLBXII) location-scale regression line equation is developed. On a given dataset, the developed model outperformed three other existing models.

Subject Classification: *(2010) 60E05, 62F10, 62E15.*

Keywords: *Location-scale, Moments, MLE, Secant-generated family, Topp-Leone-generated family, Real datasets.*

1. Introduction

Numerous disciplines, including biology, finance, engineering, insurance, quality control, and the social sciences, heavily rely on statistical distributions. Every distribution has specific characteristics of its own, including its form, range of possible values, central tendency and variability measures. The data being used and the research question being answered determine the kind of distribution that is used in a study. The modification of classical distributions to enhance their adaptability in modeling diverse datasets has garnered increasing attention. As a result, families of distributions have been created to enhance these distributions' functionality. Recently, there has been a lot of interest in trigonometric families of distributions due to their desirable properties. One such property is that they can improve distributions without increasing the number of parameters in the modified distribution that results, which solves the over-parameterization issue. From the secant function, the Secant-Generated family of distributions (Sec-G) [1] was created. When the cosine function approaches small values, the secant function can approach large values as well. Consequently, well-known distributions' shapes and tail weights are altered by the Sec-Generated family [1]. By extending the well-known Topp-Leone family of distributions, this study aims to capitalize on the favorable characteristics of the family [2]. The (STL) Family of distributions is the name given to the resulting generator. Creating a new family of distributions to enhance the properties and adaptability of special distributions is our motivation. Developing specialized distributions that can model heavy-tailed datasets is a further motivation. Furthermore, simulation experiments will be conducted to confirm the study's parameter estimation methodology [3]. Section 2 of this paper presents the derivation of the STL family. In Section 3, the Sec-G family's mixture representation is presented, and its mathematical properties are examined. Presenting the parameter estimates for the new family is the main objective of Section 4. A discussion of special distributions derived from the Sec-Generated family is given in Section 5. Section 6 deals with the Monte Carlo simulation-based validation of the parameter estimation method. The usefulness of the special distributions in actual situations is illustrated in Section 7. A novel location-scale regression model is presented in Section 8. The last section contains the study's conclusion.

2. STL Family of distributions

The TL family [2] and Sec-Generated [1] families of distributions are combined to create the STL family of distributions, which is proposed respectively.

$$Sec\left(\left(\frac{\pi}{3}G(x)\right)\right)-1 \text{ and } H(x)=G(x)^{\alpha}(1-G(x))^{\alpha}, x\in\mathbb{R}, \alpha>0$$

The (CDF) and survival functions of the STL-Generated family of distributions are obtained respectively as follows:

$$F(x)=\sec\left(\frac{\pi}{3}(1-(\bar{G}(x)^{2}))^{\alpha}\right)-1,\ \ x\in\mathbb{R}, \tag{1}$$

And

$$S(x)=2-\sec\left(\frac{\pi}{3}(1-(\bar{G}(x)^{2}))^{\alpha}\right),\ \ x\in\mathbb{R}, \tag{2}$$

α is the shape determining parameter, and $\bar{G}(x)=1-G(x)$ represents the survival function of the baseline distribution.

Equations (3) and (4) denote the PDF (Probability Density Function) and failure (hazard) rate function STL family of distributions respectively as

$$f(x)=\frac{2\pi\alpha}{3}g(x)\bar{G}(x)(1-(\bar{G}(x)^{2}))^{\alpha-1}\sec\left[\frac{\pi}{3}(1-(\bar{G}(x))^{2}))^{\alpha}\right]$$
$$\tan\left[\frac{\pi}{3}(1-(\bar{G}(x))^{2}))^{\alpha}\right], x\in\mathbb{R} \tag{3}$$

and

$$h(x)=\frac{\frac{2\pi\alpha}{3}g(x)\bar{G}(x)(1-(\bar{G}(x)^{2}))^{\alpha-1}\sec\left[\frac{\pi}{3}(1-(\bar{G}(x))^{2}))^{\alpha}\right]\tan\left[\frac{\pi}{3}(1-(\bar{G}(x))^{2}))^{\alpha}\right]}{2-\sec\left(\frac{\pi}{3}(1-(\bar{G}(x)^{2}))^{\alpha}\right)},\ \ x\in\mathbb{R}, \alpha>0. \tag{4}$$

3. Mixture representation of STL-Generated family

Here, we use a mixture representation to derive the STL-Generated family's distribution function. The mixture representation helps us to come out with the new family's statistical properties.

Lemma 1: *The mixture representation of the STL-G family is*

$$f(x)=2\alpha\sum_{k=0}^{\infty}\sum_{j=0}^{\infty}\sum_{i=0}^{\infty}w_{ijk}g(x)G(x)^{i}, \tag{5}$$

where $w_{ijk}=\dfrac{(-1)^{k+j+i}\left(\frac{\pi}{3}\right)^{2k}E_{2k}(2k)}{(2k)!}\binom{2k\alpha-1}{j}\binom{2j+1}{i}.$

Proof: Recall from the expansion of the Sec-Generated family is $\sec\left(\frac{\pi}{3}G(x)\right)$ $=\sum_{k=0}^{\infty}\frac{E_{2k}(-1)^{k}}{(2k)!}\left(\frac{\pi}{3}G(x)\right)^{2k}$, E_{2k} is known as the Euler number.

By expanding the CDF of the STL-Generated family using (1), we arrive at the following expression.

$$F(x)=\sec\left(\frac{\pi}{3}(1-(\bar{G}(x)^{2}))^{\alpha}\right)-1=\sum_{k=0}^{\infty}\frac{E_{2k}(-1)^{k}}{(2k)!}\left(\frac{\pi}{3}(1-(\bar{G}(x)^{2}))^{\alpha}\right)^{2k}-1.$$

The distribution function, PDF at this stage is given by

$$f(x)=2\alpha\sum_{k=0}^{\infty}\frac{\left(\frac{\pi}{3}\right)^{2k}E_{2k}(-1)^{k}(2k)}{(2k)!}g(x)\bar{G}(x)(1-(\bar{G}(x)^{2}))^{2k\alpha-1}. \tag{6}$$

Suppose $0<(1-G(x))^{2}<1$, then $\bar{G}(x)(1-(1-G(x))^{2})^{2k\alpha-1}$ in the PDF in equation can be expressed, using the binomial expansion twice as.

$$\bar{G}(x)(1-(1-G(x))^{2})^{2k\alpha-1}=\sum_{j=0}^{\infty}\sum_{i=0}^{\infty}(-1)^{j+i}\binom{2\alpha k-1}{j}\binom{2j+1}{i}G(x)^{i}.$$

Consequently, the PDF of the STL-G family's mixture representation is

$$f(x)=2\alpha\sum_{k=0}^{\infty}\sum_{j=0}^{\infty}\sum_{i=0}^{\infty}\frac{(-1)^{k+j+i}\left(\frac{\pi}{3}\right)^{2k}E_{2k}(-4)^{k}(2k)}{(2k)!}\binom{2k\alpha-1}{j}\binom{2j+1}{i}g(x)G(x)^{i},$$

makes the proof complete.

Equation (5) enables us to express the density of the Exponentiated-Generated (Exp-G) distribution in terms of the (PDF) of the STL-Generated family as follows:

$$f(x) = 2\alpha \sum_{k=0}^{\infty}\sum_{j=0}^{\infty}\sum_{i=0}^{\infty} w^{*}_{ijk}\,\ell_{i+1}(x), \tag{7}$$

where $w^{*}_{ijk} = \frac{w_{ijk}}{(i+1)}$ and $\ell_{i+1}(x) = (i+1)g(x)G(x)^{i}$ represent the density with power parameter (Exp-G).

4. Statistical Properties

The primary goal here is to evaluate and examine a few STL-Generated distributions' statistical properties.

4.1 *Quantile Function (QF)*

In this subsection, we derive the STL-Generated family's quantile function for simulation and derivations of other quantile based properties of the family.

Proposition 1: The STL-G random variable's quantile function can be obtained by

$$x_u = G^{-1}\left[1-\sqrt{1-\left(\frac{3}{\pi}\operatorname{arcsec}(u+1)\right)^{\frac{1}{\alpha}}}\right], \; u \in [0,1], \tag{8}$$

$G^{-1}(\cdot)$ indicates the baseline distribution's QF.

Proof: The inverse of *G* in (1) gives the QF.

4.2 *Moments and Moment Generating Functions*

4.2.1 Ordinary Moments (OM)

Proposition 2: The OM for STL-Generated family μ_r' is given by

$$\mu_r' = 2\alpha \sum_{k=1}^{\infty}\sum_{j=0}^{\infty}\sum_{i=0}^{\infty} w_{ijk} \int_{\mathbb{R}} x^{r} g(x)G(x)^{i}\,dx, \quad r = 1,2,3,\ldots \tag{9}$$

Proof: The r^{th} OM of a distribution is defined as $\mu_r' = \int_{\mathbb{R}} x^{r} f(x)dx$.

Substituting (5) for $f(x)$ in μ_r' makes the proof complete.

In terms of the quantile function, the rth ordinary moment from equation (9), can also be written as

$$\mu'_r = 2\alpha \sum_{k=0}^{\infty}\sum_{j=0}^{\infty}\sum_{i=0}^{\infty} w_{ijk} \int_0^1 Q^r{}_G(u) u^i du, \quad r = 1,2,3,... \tag{10}$$

If $u = G(x)$.

4.2.2 Incomplete Moments (IM)

Proposition 3: If $\varphi_r(t)$ represents the STL-Generated family's r^{th} incomplete moment, then

$$\varphi_r(t) = 2\alpha \sum_{k=0}^{\infty}\sum_{j=0}^{\infty}\sum_{i=0}^{\infty} w_{ijk} \int_{-\infty}^{t} x^r g(x) G(x)^i dx, r = 1,2,3,... \tag{11}$$

Proof: The r^{th} (IM) for the STL-Generated family is $\varphi_r(t) = \int_{-\infty}^{t} x^r dF(x)$. Replacing with (5) makes the proof complete.

Here is another approach to express the incomplete moment of the STL-Generated family using the concept of a quantile function.:

$$\varphi_r(t) = 2\alpha \sum_{k=0}^{\infty}\sum_{j=0}^{\infty}\sum_{i=0}^{\infty} w_{ijk} \int_0^{G(t)} Q^r{}_G(u) u^i du, \; r = 1,2,3,... \tag{12}$$

4.2.3 Moment generating function (MGF)

Proposition 4: The MGF, $M_X(t)$ of the STL-Generated family is represented as follows:

$$M_X(t) = 2\alpha \sum_{r=0}^{\infty}\sum_{k=1}^{\infty}\sum_{j=0}^{\infty}\sum_{i=0}^{\infty} \frac{w_{ijk} t^r}{r!} \int_{\mathbb{R}} x^r g(x) G(x)^i dx \;, r = 1,2,3,... \tag{13}$$

Proof: $M_X(t) = E[e^{tX}] = \int_{\mathbb{R}} e^{tx} \; dF(x)$ by definition. using $e^{tx} = \sum_{r=0}^{\infty} \frac{t^r x^r}{r!}$ [] and $M_X(t) = \sum_{r=0}^{\infty} \frac{t^r}{r!} \mu'_r$. The proof is completed by substituting the right hand side of for μ'_r here.

If $G(x) = u$, $M_X(t)$ then,

$$M_x(t) = 2\alpha \sum_{r=0}^{\infty}\sum_{k=0}^{\infty}\sum_{j=0}^{\infty}\sum_{i=0}^{\infty} \frac{w_{ijk} t^r}{r!} \int_0^1 Q^r{}_G(u) u^i du \,, r = 1,2,3,... \;, \tag{14}$$

when $M_X(t)$ is expressed with regard to quantile function.

4.3 *Mean residual life (MRL)*

Proposition 5. The STL-Generated family's (MRL) can be computed using the following formula:

$$m(t)=\frac{1}{1-F(t)}\left[\mu-2\alpha\sum_{k=0}^{\infty}\sum_{j=0}^{\infty}\sum_{i=0}^{\infty}w_{ijk}\int_{-\infty}^{t}xg(x)G(x)^{i}\,dx\right]-t. \tag{15}$$

Proof: By definition, the MRL is $m(t)=\frac{1}{1-F(t)}\left[\mu-\int_{-\infty}^{t}xf(x)dx\right]-t$. The proof is completed by substituting into the given expression for $m(t)$.

5. Parameter Estimation

The STL-Generated family's unknown parameters were estimated in this section using MLE method. Using equation (2) and parameters α and ξ, and given a random sample of size , the following is an expression for the log-likelihood function:

$$\begin{aligned}\ell=&\,n\log\left(\frac{2\pi}{3}\right)+n\log(\alpha)+\sum_{i=1}^{n}\log g(x_i;\xi)+\sum_{i=1}^{n}\log(1-G(x_i;\xi))\\&+(\alpha-1)\sum_{i=1}^{n}\log(1-(1-G(x_i;\xi)^2)+\sum_{i=1}^{n}\log\left\{\sec\left(\frac{\pi}{3}(1-(1-G(x_i;\xi))^2)^{\alpha}\right)\right\}\\&+\sum_{i=1}^{n}\log\left\{\tan\left(\frac{\pi}{3}(1-(1-G(x_i;\xi))^2)^{\alpha}\right)\right\},\ x\in\mathbb{R}.\end{aligned} \tag{16}$$

Equation (16) presents the log-likelihood function, which is maximized to derive the parameter estimates obtained from the MLE method. These parameters can be obtained using statistical software, R. For the purpose of this work, the statistical program R was employed.

6. Five distinct distributions of the STL-Generated family

In this section, the STL-Generated family of distributions is extended to five existing distributions.

6.1 *STL- Chen*

We introduce the STL-Chen (STLCh) distribution. We also look into how its hazard and density functions behave. Assuming the Chen distribution [4] as the baseline distribution, its CDF as well as PDF are as follows: $G(x)=1-e^{\beta(1-e^{x^{\lambda}})}$ and $g(x)=\lambda\beta x^{\lambda-1}\,e^{(\beta(1-e^{x^{\lambda}})+x^{\lambda})}$, $x>0,\ \lambda>0,\ \beta>0$ respectively.

The STL-Chen (STLCh) distribution's CDF, PDF, and hazard rate (HR) function are

$$F(x)=\sec\left[\frac{\pi}{3}(1-e^{2\beta(1-e^{x^{\lambda}})})^{\alpha}\right]-1,\ x>0,\lambda>0,\beta>0,\alpha>0, \tag{17}$$

$$f(x)=\frac{2\pi\beta\lambda\alpha}{3}x^{\lambda-1}e^{2\beta(1-e^{x^{\lambda}})}e^{x^{\lambda}}(1-e^{2\beta(1-e^{x^{\lambda}})})^{\alpha-1}\sec\left[\frac{\pi}{3}(1-e^{2\beta(1-e^{x^{\lambda}})})^{\alpha}\right]$$
$$\tan\left[\frac{\pi}{2}(1-e^{2\beta(1-e^{x^{\lambda}})})^{\alpha}\right],x>0, \tag{18}$$

and

$$h(x)=\frac{\frac{2\pi\beta\lambda\alpha}{3}x^{\lambda-1}e^{2\beta(1-e^{x^{\lambda}})}e^{x^{\lambda}}(1-e^{2\beta(1-e^{x^{\lambda}})})^{\alpha-1}\sec\left[\frac{\pi}{3}(1-e^{2\beta(1-e^{x^{\lambda}})})^{\alpha}\right]\tan\left[\frac{\pi}{3}(1-e^{2\beta(1-e^{x^{\lambda}})})^{\alpha}\right]}{2-\sec\left[\frac{\pi}{2}(1-e^{-2\lambda x^{\beta}})^{\alpha}\right]},x>0,$$

respectively.

The plots of the STLCh (PDF) and (HRF) are shown in Figure 1. Various shapes, including symmetric, decreasing, left- and left-skewed, are displayed in the PDF plot according to the selected parameter values. The HRF plot, on the other hand, displays clear patterns, such as bathtub-shaped, increasing, and decreasing failure rates.

Given below is the STLCh distribution's quantile function:

$$x_u=\left[\log\left(1-\left(\beta^{-1}\log\left(\sqrt{1-\left(\frac{3}{\pi}\operatorname{arcsec}(u+1)\right)^{\frac{1}{\alpha}}}\right)\right)\right)\right]^{\frac{1}{\lambda}},0\le u\le 1. \tag{20}$$

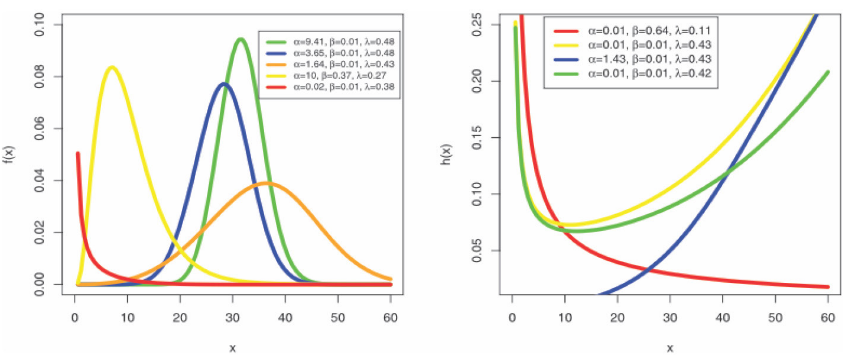

Figure 1

A selection of the density and hazard function curves for the STLCh distribution

6.2 *STL Weibull Distribution*

The STL-Weibull (STLW) distribution is developed using the Weibull distribution as a baseline, which was first presented by [5]. The CDF and PDF of the Weibull distribution are defined as follows: $G(x) = 1 - e^{-\lambda x^{\beta}}$ and $g(x) = \lambda\beta x^{\beta-1}\, e^{-\lambda x^{\beta}}$, $x > 0,\ \lambda > 0,\ \beta > 0.$

The STLW distribution's CDF and PDF are given respectively as

$$F(x) = \sec\left[\frac{\pi}{3}(1 - e^{-2\lambda x^{\beta}})^{\alpha}\right] - 1,\ x > 0, \lambda > 0, \beta > 0, \alpha > 0 \tag{21}$$

and

$$f(x) = \frac{2\pi\alpha\lambda\beta}{3} x^{\beta-1} e^{-2\lambda x^{\beta}} (1 - e^{-2\lambda x^{\beta}})^{\alpha-1} \sec\left[\frac{\pi}{3}(1 - e^{-2\lambda x^{\beta}})^{\alpha}\right] \tan\left[\frac{\pi}{3}(1 - e^{-2\lambda x^{\beta}})^{\alpha}\right],\ x > 0. \tag{22}$$

The failure rate of the STLW distribution is

$$h(x) = \frac{\frac{2\pi\alpha\lambda\beta}{3} x^{\beta-1} e^{-2\lambda x^{\beta}} (1 - e^{-2\lambda x^{\beta}})^{\alpha-1} \sec\left[\frac{\pi}{3}(1 - e^{-2\lambda x^{\beta}})^{\alpha}\right] \tan\left[\frac{\pi}{3}(1 - e^{-2\lambda x^{\beta}})^{\alpha}\right]}{2 - \sec\left[\frac{\pi}{3}(1 - e^{-2\lambda x^{\beta}})^{\alpha}\right]},\ x > 0.$$

The density and hazard rate plots of the STLW distribution for a range of parameter values is shown in Figure 2. Whereas the hazard rate plots show bathtub, upside-down bathtub, and decreasing failure rates, the density plot displays decreasing and right-skewed shapes.

The QF of the STLW distribution is given as

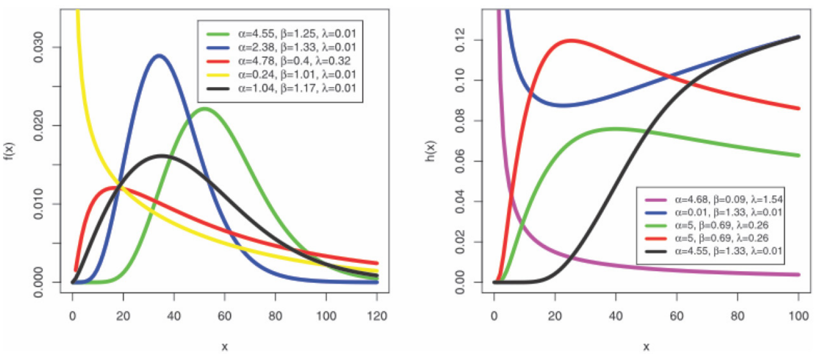

Figure 2

Density and HR plots of the STLW distribution

$$x_u = \left[-\lambda^{-1} \log\left(\sqrt{1-\left(\frac{3}{\pi}\operatorname{arcsec}(u+1)\right)^{\frac{1}{\alpha}}} \right) \right]^{\frac{1}{\beta}}, 0 \le u \le 1. \tag{24}$$

6.3 *STL Burr III*

The CDF of the Burr III distribution [6], $G(x) = (1+x^{-\beta})^{-\lambda}$ and $x>0$, $\beta>0$ is the baseline distribution of the developed STL-Burr III (STLB) distribution. Consequently, the CDF, PDF and the HR functions of the STLBIII distribution are given respectively as

$$F(x) = \sec\left[\frac{\pi}{3}(1-(1-[1+x^{-\beta}]^{-\lambda})^2)^{\alpha}\right]-1, x>0, \lambda>0, \beta>0, \alpha>0, \tag{25}$$

$$f(x) = \frac{2\pi\alpha\beta\lambda}{3} x^{-\beta-1}[1+x^{-\beta}]^{-\lambda-1}(1-[1+x^{-\beta}]^{-\lambda})(1-(1-[1+x^{-\beta}]^{-\lambda})^2)^{\alpha-1} \\ \times \sec\left[\frac{\pi}{3}(1-(1-[1+x^{-\beta}]^{-\lambda})^2)^{\alpha}\right]\tan\left[\frac{\pi}{3}(1-(1-[1+x^{-\beta}]^{-\lambda})^2)^{\alpha}\right], x>0 \tag{26}$$

and

$$h(x) = \frac{\frac{2\pi\alpha\beta\lambda}{3} x^{-\beta-1}[1+x^{-\beta}]^{-\lambda-1}(1-[1+x^{-\beta}]^{-\lambda})(1-(1-[1+x^{-\beta}]^{-\lambda})^2)^{\alpha-1} \times \sec\left[\frac{\pi}{3}(1-(1-[1+x^{-\beta}]^{-\lambda})^2)^{\alpha}\right]\tan\left[\frac{\pi}{3}(1-(1-[1+x^{-\beta}]^{-\lambda})^2)^{\alpha}\right]}{2-\sec\left[\frac{\pi}{3}(1-(1-[1+x^{-\beta}]^{-\lambda})^2)^{\alpha}\right]}, x>0. \tag{27}$$

Figure 3 displays the density plot of the STLB distribution, which demonstrates forms of reversed-J and right-skew. The HRF plot of the

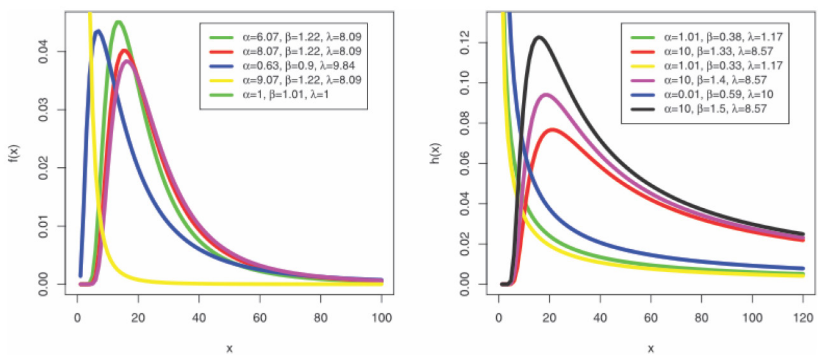

Figure 3

Plots of the density function and HRF of STLB distribution

STLB distribution also in Figure 3 illustrates shapes of a decreasing and upside-down bathtub.

The QF x_u for the Secant Topp-Leone Burr III Distribution is given by

$$x_u = \left(\left(1 - \sqrt{1 - (\tfrac{3}{\pi} \operatorname{arcsec}(u+1))^{\frac{1}{\alpha}}} \right)^{-\frac{1}{\lambda}} - 1 \right)^{-\frac{1}{\beta}}, 0 \le u \le 1. \tag{28}$$

6.4 *STI- Lomax Distribution*

The Lomax distribution [17] served as the foundation for the development of the STL-Lomax (STLLx) distribution. The Lomax distribution's CDF and PDF are, respectively, $G(x) = 1 - \left(1 + \frac{x}{\lambda}\right)^{-\beta}$ and $g(x) = \frac{\beta}{\lambda}\left[1 + \frac{x}{\lambda}\right]^{-(\beta+1)}$, $x > 0, \lambda > 0, \beta > 0.$

The CDF of the STLLx distribution is derived when we substitute the CDF of the Lomax distribution for the CDF of the STL-Generated family. The resulting CDF of the STLLx distribution function is presented as

$$F(x) = \sec\left[\frac{\pi}{3}\left(1 - \left(1 + \frac{x}{\lambda}\right)^{-2\beta}\right)^{\alpha}\right] - 1. \tag{29}$$

The PDF of the STLLx distribution is also given as

$$f(x) = \frac{2\pi\alpha}{3}\left(\left(\frac{\beta}{\lambda}\left(1 + \frac{x}{\lambda}\right)\right)^{-(\beta+1)}\right)\left(\left(1 + \frac{x}{\beta}\right)^{-\beta}\right)\left(\left(1 - \left(1 + \frac{x}{\lambda}\right)^{-2\beta}\right)^{\alpha-1}\right)$$
$$\times \sec\left[\frac{\pi}{3}\left(1 - \left(1 + \frac{x}{\lambda}\right)^{-2\beta}\right)^{\alpha}\right] \tan\left[\frac{\pi}{3}\left(1 - \left(1 + \frac{x}{\lambda}\right)^{-2\beta}\right)^{\alpha}\right], x > 0. \tag{30}$$

With the failure rate function,

$$h(x) = \frac{\frac{2\pi\alpha}{3}\left(\left(\frac{\beta}{\lambda}\left(1 + \frac{x}{\lambda}\right)\right)^{-(\beta+1)}\right)\left(\left(1 + \frac{x}{\beta}\right)^{-\beta}\right)\left(\left(1 - \left(1 + \frac{x}{\lambda}\right)^{-2\beta}\right)^{\alpha-1}\right) \times \sec\left[\frac{\pi}{3}\left(1 - \left(1 + \frac{x}{\lambda}\right)^{-2\beta}\right)^{\alpha}\right] \tan\left[\frac{\pi}{3}\left(1 - \left(1 + \frac{x}{\lambda}\right)^{-2\beta}\right)^{\alpha}\right]}{2 - \sec\left[\frac{\pi}{3}\left(1 - \left(1 + \frac{x}{\lambda}\right)^{-2\beta}\right)^{\alpha}\right]}, x > 0. \tag{31}$$

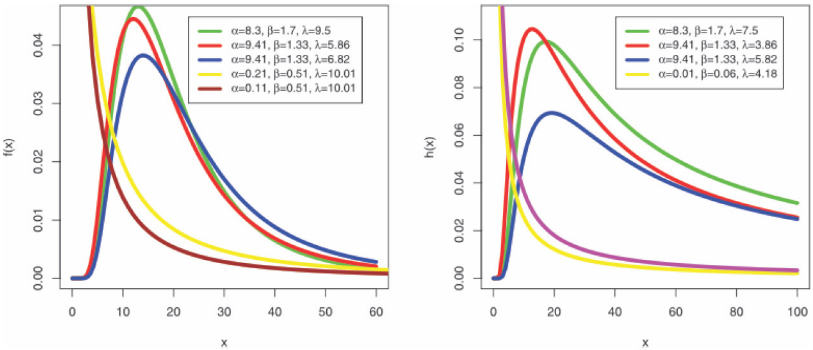

Figure 4

Plots of density and hazard rate functions of *S*TLLx distribution

Figure 4 depicts the density plot of the STLLx distribution, showcasing shapes characterized by decreasing and right-skew tendencies. Additionally, Figure 4 also presents the failure rate plot of the STLLx revealing patterns, the upside-down bathtub shapes and failure rate functions decreasing.

The QF x_u for the STLLx distribution is given by

$$x_u = \left(\lambda \left(\left(\sqrt{1-\left(\frac{3}{\pi}\operatorname{arcsec}(u+1)\right)^{\frac{1}{\alpha}}} \right)^{-\frac{1}{\beta}} - 1 \right) \right), 0 \le u \le 1. \tag{32}$$

4.6.3. STL BXII Distribution

Using the BXII distribution [6], the STLBXII is obtained. The CDF and PDF are respectively, given as

$$G(x) = 1-\left[1+\left(\frac{x}{\lambda}\right)^c\right]^{-\beta} \text{ and } g(x) = \frac{c\beta}{\lambda}\left(\frac{x}{\lambda}\right)^{c-1}\left[1+\left(\frac{x}{\lambda}\right)^c\right]^{-(\beta+1)}, \; x>0, \; \lambda>0,$$

$c>0, \; \beta>0$ as the baseline distribution.

The CDF and PDF of the STLBXII distribution are respectively,

$$F(x) = \sec\left[\frac{\pi}{3}\left[1-\left(1+\left(\frac{x}{\lambda}\right)^c\right)^{-2\beta}\right]^{\alpha}\right] - 1, x>0, \lambda>0, c>0, \beta>0, \alpha>0 \tag{33}$$

and

$$f(x)=\frac{2\pi\alpha c\beta}{3\lambda}\left(\frac{x}{\lambda}\right)^{c-1}\left[1+\left(\frac{x}{\lambda}\right)^{c}\right]^{-(2\beta+1)}\left[1-\left(1+\left(\frac{x}{\lambda}\right)^{c}\right)^{-2\beta}\right]^{\alpha-1}$$
$$\times\sec\left[\frac{\pi}{3}\left(1-\left(1+\left(\frac{x}{\lambda}\right)^{c}\right)^{-2\beta}\right)^{\alpha}\right]\tan\left[\frac{\pi}{3}\left(1-\left(1+\left(\frac{x}{\lambda}\right)^{c}\right)^{-2\beta}\right)^{\alpha}\right], x>0. \quad (34)$$

The STLBXIII distribution's failure rate function is given by

$$h(x)=\frac{\frac{2\pi\alpha c\beta}{3\lambda}\left(\frac{x}{\lambda}\right)^{c-1}\left[1+\left(\frac{x}{\lambda}\right)^{c}\right]^{-(2\beta+1)}\left[1-\left(1+\left(\frac{x}{\lambda}\right)^{c}\right)^{-2\beta}\right]^{\alpha-1}\times\sec\left[\frac{\pi}{3}\left(1-\left(1+\left(\frac{x}{\lambda}\right)^{c}\right)^{-2\beta}\right)^{\alpha}\right]\tan\left[\frac{\pi}{3}\left(1-\left(1+\left(\frac{x}{\lambda}\right)^{c}\right)^{-2\beta}\right)^{\alpha}\right]}{2-\sec\left[\frac{\pi}{3}\left(1-\left(1+\left(\frac{x}{\lambda}\right)^{c}\right)^{-2\beta}\right)^{\alpha}\right]}, x>0. \quad (35)$$

Figure 5 demonstrates the density plot of the STLBXIII distribution, with different parameter values and figure 6 presents the hazard rate plot of the STLBXIII distribution

The QF of the STLBXII distribution is given by

$$x_u=\left[\lambda^{c}\left(\left(\sqrt{1-\left(\frac{3}{\pi}\operatorname{arcsec}(u+1)\right)^{\frac{1}{\alpha}}}\right)^{-\frac{1}{\beta}}-1\right)\right]^{\frac{1}{c}}, 0\le u\le 1.$$

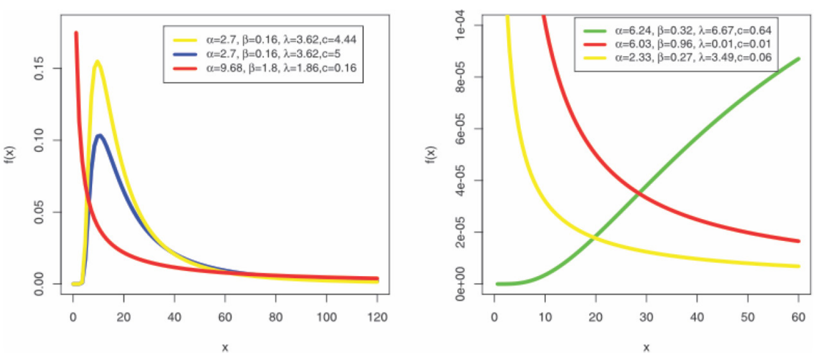

Figure 5

Plots of the density function of STLBXII distribution

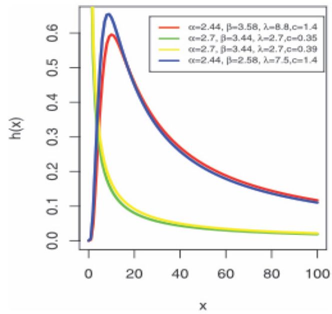

Figure 6

Plot of HF of STLBXII distribution

7. Simulation

To assess the efficacy of MLE technique in parameter estimation for different sample sizes, we performed Monte Carlo simulations with the STLCh distribution in this section. , and sample sizes were generated for the chosen parameters. $\mathrm{I}:\alpha=1.4,\ \beta=2.5,\ \lambda=3.8$ and $\mathrm{II}:\alpha=0.4,\ \beta=1.5,\ \lambda=1.8,$ and repeated the simulation 3000 times for each sample. We evaluated coverage probability (CP), average width (AW), root mean square error (RMSE), and average bias (AB) at a 95% confidence level in order to assess how well the parameter estimators performed. The results of this evaluation are presented in Table 1. Note that as the sample size increased, AB and root mean square error RMSE decreased towards zero in all cases. Additionally, the AW became narrower. These results imply that there is a greater chance of obtaining unbiasedness and consistency of MLE estimators with larger sample sizes. Therefore, the maximum likelihood technique is deemed to be an effective parameter estimator for the STLCh distribution.

Table 1

Simulation results for STLCh

Parameter	n	I				II			
		AB	RMSE	CP	AW	AB	RMSE	CP	AW
α	25	1.606	2.753	0.999	18.797	0.535	1.611	0.931	5.935
	75	0.802	1.697	0.999	7.632	0.093	0.413	0.911	1.258
	100	0.714	1.528	0.999	6.289	0.061	0.290	0.917	0.956
	150	0.463	1.086	0.999	4.260	0.032	0.188	0.921	0.690
	200	0.358	0.893	0.999	3.370	0.018	0.152	0.918	0.566

Contd...

β	25	0.146	0.498	0.991	2.747	0.464	0.848	0.985	3.673
	75	0.019	0.275	0.982	1.424	0.139	0.354	0.986	1.193
	100	0.035	0.234	0.983	1.242	0.119	0.295	0.977	0.967
	150	0.006	0.197	0.979	1.002	0.063	0.201	0.977	0.695
	200	0.001	0.174	0.973	0.865	0.046	0.165	0.978	0.581
λ	25	-0.409	0.867	0.967	8.511	0.536	1.333	0.913	7.679
	75	-0.315	0.710	0.949	4.950	0.224	0.826	0.935	3.244
	100	-0.290	0.665	0.947	4.306	0.189	0.725	0.946	2.699
	150	-0.228	0.572	0.951	3.550	0.121	0.541	0.956	2.007
	200	-0.196	0.513	0.954	3.083	0.102	0.471	0.956	1.690

8. Application

In this section, we compared the developed models to existing distributions in order to conduct a practical application analysis. We used a variety of accuracy measures, such as the log-likelihood (LL), along with information criteria measures, like the Hannan-Quinn information criterion, the Bayesian information criterion (BIC), corrected Akaike information criterion, and Akaike information criterion (AIC), to evaluate the performance of our models. In addition, we compared the models using goodness-of-fit (GF) measures like the Cramér-von Mises (CM), Kolmogorov-Smirnov (KS) and Anderson-Darling (AD) tests. The best model was determined by taking into account the highest log-likelihood value, the smallest values of these measures. We used the R statistical software and the “mle2” subroutine from the “bbmle” package for parameter estimation and log-likelihood function optimization [7].

The developed secant Topp-Leone Burr III (STLB) distribution was compared to well-known distributions such as Chen (CHEN) [4], Gumbel (GUM) [8], Exponentiated Inverse Flexible Weibull Extension (EINFW) [9], Nakagami (NAK) [10], Generalized Inverse Weibull (GINW) [11], Cauchy (Ca) [12], and Inverted Exponential (IE) [13] distributions.

8.1 *First Application*

The survival times of 172 patients waiting for heart transplants at Stanford University serve as the dataset used in this application. It is contained in [15] and [14] of R’s survival package. The least and highest times of survival, according to the dataset, were 1 and 1800 days, respectively. 201.30 was the average survival duration, with a standard deviation of 358.07. The skewness value of 2.53 suggested a right-skewed distribution, and the kurtosis value of 16.10 suggested a heavy-tailed distribution. Table 2 displays parameter estimations for the given dataset across various models, along with their corresponding SEs (in parenthesis). Table 3 indicates that the STLB distribution gives the best performance.

Table 2

Parameter estimates and standard errors of models for heart data

Model	α	β	λ
STLB	0.151(0.140)	0.572(0.061)	20.221(18.199)
CHEN	0.076(0.011)	0.195(0.006)	
GUM	77.27(12.454)	159.808(11.415)	
EINFW	1.988(0.191)	0.004(0.001)	1.054(0.098)
NAK	9418(1.65e-08)	0.04843(3.78e-03)	
GINW	2.907(0.124)	0.586(0.032)	3.195(0.193)
Ca	33.279(3.936)	31.792(3.617)	
IE	12.494(0.953)		

Table 3

Various statistical measures of competing models for heart data

Model	**LL**	**AIC**	**CAIC**	**BIC**	**HQIC**	**CM**	**AD**	**KS**
STLB	-1020.710	2047.410	2047.550	2056.850	18.523	0.088	0.683	**0.049**
CHEN	-1048.350	2100.710	2100.780	2107.000	18.576	0.981	5.946	0.145
GUM	-1177.960	2359.920	2359.990	2366.220	18.809	3.846	22.001	0.283
EINFW	-1069.990	2145.970	2146.110	2155.410	18.617	1.712	8.874	0.202
NAK	-1258.170	2520.330	2520.380	2526.630	18.940	23.612	130.770	0.591
GINW	-1029.910	2065.820	2065.970	2072.260	18.541	0.315	2.136	0.094
Ca	-1107.440	2218.890	2218.990	2225.180	18.686	3.319	26.115	0.248
IE	-1090.930	2183.860	2183.880	2187.010	18.656	6.477	39.782	0.302

Figure 7 which displays the fitted CDF plots of the competing distributions shows that the developed STLB distributions' CDF mimics the empirical CDF of heart transplant data.

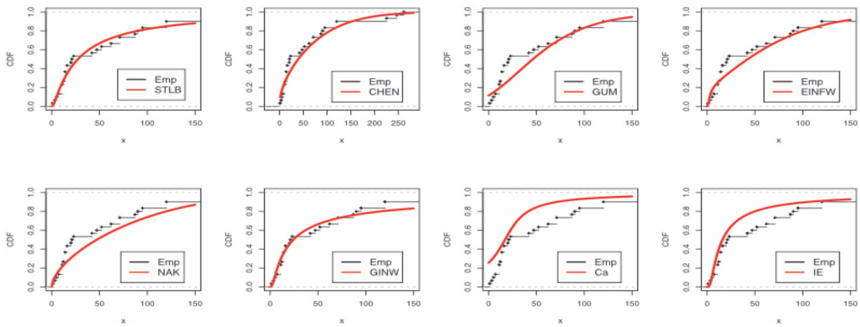

Figure 7

Graphs of CDF fitted competing distributions for airplane data

8.2 *Second Application*

The data used for this analysis concerns the failure time of an airplane air conditioning system. The dataset is available in [16]. The data analysis reveals that the lowest and highest failure times are 1 and 261 respectively. The average failure time is 59.6, the standard deviation of 71.88 and the skewness value is 1.61, a moderately right-skewed distribution, while the kurtosis value is 1.64, suggesting a slightly heavy-tailed distribution. The parameter estimates and their SEs (in parentheses) for the different competing models are presented in Table 4. Based on the log-likelihood, information criteria, and goodness-of-fit measures are shown in Table 5, it is evident that the STLB distribution outperforms the other known distributions.

Table 4

Estimates of parameter values and SEs of models for the air-conditioning of airplane data

	α	β	λ
STLB	**0.208(0.396)**	**0.708(0.157)**	**17.957(32.597)**
CHEN	0.052(0.019)	0.265(0.019)	
GUM	31.353(7.681)	40.615(6.569)	
EINFW	1.251(0.441)	0.019(0.004)	1.520(0.362)
NAK	9418.000(6.39 $\times 10^{-7}$)	0.295(0.060)	
GINW	4.501(341.367)	0.724(0.093)	2.346(128.774)
Ca	17.139(6.329)	17.689(4.761)	
IE	11.179(2.041)		

Table 5

Statistical measures of models for the airplane air-conditioning data

Model	ℓ	AIC	CAIC	BIC	HQIC	CM	AD	KS
STLB	**-152.282**	**310.627**	**311.487**	**314.767**	**13.906**	**0.069**	**0.432**	**0.116**
CHEN	-154.390	312.780	313.225	315.583	13.933	0.132	0.881	0.151
GUM	-161.982	327.964	328.408	330.766	14.028	0.279	1.880	0.241
EINFW	-155.014	316.027	316.950	320.231	13.941	0.145	0.927	0.177
NAK	-153.731	311.461	311.758	314.964	13.918	0.225	1.189	0.203
GINW	-155.114	316.229	317.152	320.432	13.942	0.106	0.786	0.159
Ca	-164.792	333.583	334.250	336.386	14.087	0.858	5.382	0.270
IE	-159.062	320.124	320.267	321.525	13.992	0.486	2.822	0.233

The CDF plots of the parametric fit of the competing distributions in Figure 8 provide visual evidence that the STLB distribution provides a good parametric fit to the failure time data of the air-conditioning system of an airplane.

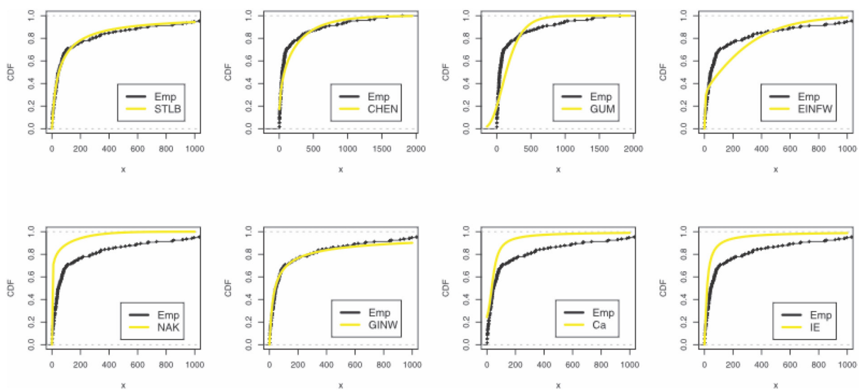

Figure 8

Graphs of fitted distributions of competing models for heart data

9. The Log STLBXII Location-scale equation of regression line

From the STLBXII distribution, a new location-scale regression line equation called log-STLBXII (LSTLBXII) was developed. Applying the logarithmic transformation to the response variable, where $Y = \ln(X)$ and taking into consideration a location-scale re-parametrization with $\lambda = e^{\mu}$

and $c = 1/\sigma$ yields the LSTLBXII regression model. Taking into consideration that the STLBXII distribution's CDF given, $F_Y(y) = P(Y \le y)$, but $Y = \ln(X)$. Therefore $F_Y(y) = P(X \le e^y)$. Thus

$$F_Y(y) = \sec\left[\frac{\pi}{3}\left(1-\left(1+\left(e^{\left(\frac{y-\mu}{\sigma}\right)}\right)\right)^{-2\beta}\right)^{\alpha}\right]-1, y \in \mathbb{R}. \tag{36}$$

$\sigma > 0, \alpha > 0, \gamma > 0, \beta > 0, \mu \in \mathbb{R}$ and $y \in \mathbb{R}$.

Another way to express the LSTLBXII regression model's survival function is as

$$S_Y(y) = 2-\sec\left[\frac{\pi}{3}\left(1-\left(1+\left(e^{\left(\frac{y-\mu}{\sigma}\right)}\right)\right)^{-2\beta}\right)^{\alpha}\right], y \in \mathbb{R}. \tag{37}$$

Consequently, the PDF of LSTLBXII, $f_Y(y)$ can be written as

$$f_y(y) = \frac{2\pi\alpha\beta}{3\sigma} e^{\left(\frac{y-\mu}{\sigma}\right)}[1+(e^{\left(\frac{y-\mu}{\sigma}\right)})]^{-(2\beta+1)}[1-(1+(e^{\left(\frac{y-\mu}{\sigma}\right)}))^{-2\beta}]^{\alpha-1}$$
$$\left(\sec\left[\frac{\pi}{3}[1-(1+(e^{\left(\frac{y-\mu}{\sigma}\right)}))^{-2\beta}]^{\alpha}\right]\right)\times\left(\tan\left[\frac{\pi}{3}[1-(1+(e^{\left(\frac{y-\mu}{\sigma}\right)}))^{-2\beta}]^{\alpha}\right]\right), \ y \in \mathbb{R}. \tag{38}$$

Given that $z = (y-\mu)/\sigma$, then the standardized random variable's PDF is

$$f_y(y;\alpha,\gamma,\beta,\mu,\sigma) = \frac{2\pi\alpha\beta}{3\sigma}\exp(z)[1+(\exp(z))]^{-(2\beta+1)}[1-(1+(\exp(z)))^{-2\beta}]^{\alpha-1}$$
$$\left(\sec\left[\frac{\pi}{3}[1-(1+(\exp(z)))^{-2\beta}]^{\alpha}\right]\right)\times\left(\tan\left[\frac{\pi}{3}[1-(1+(\exp(z)))^{-2\beta}]^{\alpha}\right]\right), \ y \in \mathbb{R}. \tag{39}$$

Using the LSTLBXII density, a new location-scale regression model is presented, where the regression structure is

$$y_i = \mathbf{x_i}^T\beta + \sigma z_i, i = 1,\dots,n, \tag{40}$$

where, in equation (40), z_i is the random error that follows the density and $\mathbf{x}_i^T$ is the independent variable vector. The location parameter, $\mu_i = \mathbf{x}_i^T\beta$ is represented by the regression parameters, $\beta = (\beta_1,\dots,\beta_p)^T$.

The MLE method was used to estimate the unknown parameters of the LSTLBXII regression model. In equation (40), the dependent variable is denoted by y_i and is distributed as LSTLBXII.

In this context, the response variable, defined as $y_i = \min\{\ln(x_i), \ln(c_i)\}$. The expressions $\ln(x_i)$ and $\ln(c_i)$ correspond to the log lifetime and log censoring times, respectively. The dataset is divided into two groups:. Individuals having log-censoring and log-lifetime are represented by F and C, respectively. These definitions allow us to express the log-likelihood function of the LSTLBXII regression line equation as

$$\ell(\tau) = r\left(\frac{2\pi\alpha\beta}{3\sigma}\right)\sum_{i\in F} z_i - (2\beta+1)\sum_{i\in F}\log(1+(\exp(z_i))) + (\alpha-1)\sum_{i\in F}\log(1-(1+(\exp(z_i)))^{-2\beta})$$
$$+\sum_{i\in F}\log\left(\sec\left[\frac{\pi}{3}[1-(1+(\exp(z_i)))^{-2\beta}]^{\alpha}\right]\right) + \sum_{i\in F}\log\left(\tan\left[\frac{\pi}{3}[1-(1+(\exp(z_i)))^{-2\beta}]^{\alpha}\right]\right)$$
$$+\sum_{i\in C}\log\left(2-\sec\left[\frac{\pi}{3}(1-(1+(\exp(z_i)))^{-2\beta})^{\alpha}\right]\right),$$

where $\tau = (\alpha, \beta, \sigma, B^T)$ is the parameter vector, $z_i = (y_i - x_i^T\beta)/\sigma$ and is the total number of observations that are uncensored. Maximizing the log-likelihood function in equation (41) yields MLEs.

This study used a real-life dataset of infection recurrence times in patients numbering 76 who had kidney issues using portable dialysis equipment to show how the developed LSTLBXII regression model could be applied. The dataset was sourced from McGilchrist and Aisbett's (1991) work and was obtained using the R software's survival package. The censoring rate of the dataset was roughly 24%. The study's response variable was the patients' time of recurrence, which was denoted as (y_i). The explanatory variables included the age of patients (x_{i2}), frailty estimate of patients (x_{i2}), and sex of patients (x_{i3}). The log-Lomax-Weibull (LLW) regression model, which was proposed by [17], the log-generalized inverse-Weibull (LGIW) regression line equation, which was introduced by [11], and the log-Topp-Leone Weibull (LTLW) regression line equation, which was presented by [18], were the models that were used to compare the performance of the LSTLBXII regression line equation. It is necessary to fit the regression line equation listed below:

$$y_i = \beta_0 + \beta_1 x_{i1} + \beta_2 x_{i2} + \beta_3 x_{i3} + \sigma z_i, \tag{42}$$

where y_i is distributed as LSTLBXII.

Table 6 provides the parameter estimates and measures of goodness-of-fit for the competing models, showing that the LSTLBXII model has the minimum of AIC, BIC, and CAIC values, indicating that it is the most suitable model. The results also revealed that from the developed LSTLBXII regression model, the chance of kidney infection increases with increase in age although insignificant at 5% level. An increase in frailty estimate also increases the chance of kidney infection (*p-value* < 0.05). As well,

Table 6

Goodness-of-fit indicators and regression parameters

Distribution	Parameters	Estimates	SEs	P-values	Goodness-of-fit
LSTLBXII	B0	11917.000	3.91×10^{-2}	< 0.0001	AIC=1473.787
	B1	8.067	4.59×10^{-3}	0.7540	
	B2	7197.000	1.35	< 0.0001	BIC=1490.102
	B3	17701.000	2.38×10^{-1}	< 0.0001	
	α	4.058	1.15	< 0.0001	
	β	4.273	7.11×10^{-1}	< 0.0001	CAIC=1474.644
	σ	111240.000	1.28	< 0.0001	
LGIW	B0	1101000.000	1.05×10^{-7}	< 0.0001	AIC=1765.533
	B1	-23064.000	4.00×10^{-6}	< 0.0001	
	B2	9000.000	1.30×10^{-7}	< 0.0001	BIC=1779.518
	B3	1.000	7.34×10^{-8}	< 0.0001	
	α	0.973	1.16×10^{-1}	< 0.0001	CAIC=1767.682
	σ	1100000.000	2.22×10^{-8}	< 0.0001	
LLW	B0	452110.000	3.15×10^{-9}	< 0.0001	AIC=1547.922
	B1	1926.900	1.28×10^{-7}	< 0.0001	
	B2	89985.000	2.86×10^{-9}	< 0.0001	BIC=1564.237
	B3	162220.000	1.27×10^{-7}	< 0.0001	
	α	49.044	6.53×10^{-6}	< 0.0001	CAIC=1549.569
	β	0.049	6.48×10^{-4}	< 0.0001	
	σ	100010.000	2.13×10^{-8}	< 0.0001	
LTLW	B0	97.093	8.81×10^{-12}	< 0.0001	AIC=1495.381
	B1	3987.800	4.24×10^{-8}	< 0.0001	
	B2	-3.1094.000	1.04×10^{-11}	< 0.0001	BIC=1511.696
	B3	-4.3341.000	5.43×10^{-12}	< 0.0001	
	α	142.120	6.22×10^{-9}	< 0.0001	
	θ	0.002	3.20×10^{-4}	< 0.0001	CAIC=1497.028
	σ	10052.000	1.68×10^{-10}	< 0.0001	

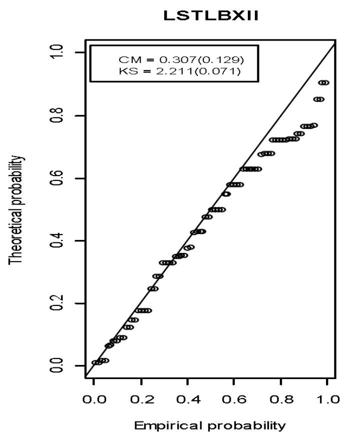

Figure 9

Cox-Snell plot of residuals of fitted regression equation

chance of kidney infection among women patients was higher than that of the male patients (*p-value* < 0.05).

The LSTLBXII regression model's adequacy was investigated and for the kidney infection dataset. This was done by estimating their residuals due to Cox-Snell [19] and also their goodness-of-fit measures.

The residual due to Cox and Snell is

$$\hat{r}_i = -\ln \hat{S}(y_i / x_i), \tag{43}$$

$\hat{S}(\cdot)$ is the estimated survival function in this case. A model fits data adequately provided the residuals (Cox-Snell) follow an exponential distribution with a unit parameter [19].

The goodness of fit of the LSTLBXIII model to the dataset is illustrated in Figure 9, which shows the Cox-Snell residual plot. The plotted points in the plot are found to be closer to the diagonal line, indicating a satisfactory fit of the model to the dataset. This visual observation is further supported by the goodness-of-fit measures and their associated probability-values provided in Table 6.

10. Conclusions

In this research, a completely new generated family of distributions, known as the STL-Genreated family, is introduced. The study establishes various mathematical properties. The STL family encompasses several distinct distributions, each possessing unique characteristics. These include the following distributions: STL Chen, STLW, secant STLBIII, STLL, and STLBXI . These distributions exhibit desirable shapes and failure rate plots, making them valuable tools in modeling various phenomena and analyzing data.

The MLE technique is used to estimate the parameters, and Monte Carlo simulation experiments are performed to validate the adequacy of the estimates. The developed models are shown to be applicable using two real-lifed datasets from the fields of aviation and health. Using goodness-of-fit tests, the STLBIII outperforms seven distributions. Additionally, a new LSTLBXII regression model is developed from the STLBXII distribution, and it outperforms the LGIW, LLW and LTLW regression models according to goodness-of-fit tests. The assessment of the suitability of the developed models was done by using Cox-Snell residuals. Overall, the developed models provide better parametric fits for the given datasets.

References

[1] L. Souza, W. R. de Oliveira, C. C. R. de Brito, C. Chesneau, R. Fernandes, and T. A. E. Ferreira, "Sec-G Class of Distributions: Properties and Applications," *Symmetry,* vol. 14, no. 2, Art. no. 299 (2022), doi: 10.3390/sym14020299.

[2] A. Al-Shomrani, O. Arif, A. Shawky, S. Hanif, and M. Q. Shahbaz, "Topp-Leone family of distributions: Some properties and application," *Pakistan Journal of Statistics and Operation Research*, vol. 12, no. 3, pp. 443–451 (2016).

[3] D. Rahardja, H. Wu, Z. Zhang, and A. D. Tiedt, "Maximum likelihood estimation for the proportion difference of two-sample binomial data subject to one type of misclassification," *Journal of Statistics and Management Systems*, vol. 22, no. 8, pp. 1365-1379 (2019), doi: 10.1080/09720510.2019.1606319.

[4] Z. Chen, "A new two-parameter lifetime distribution with bathtub shape or increasing failure rate function," *Statistics and Probability Letters*, vol. 49, no. 2, pp. 155–161 (2000), doi: 10.1016/s0167-7152(00)00044-4.

[5] W. Weibull, "Statistical theories of the strength of materials," Royal British Institute of Engineering, vol. 51, pp. 189–206 (1939).

[6] I. W. Burr, "Cumulative Frequency Functions," *The Annals of Mathematical Statistics*, vol. 13, pp. 215-232 (1942), doi: 10.1214/aoms/1177731607.

[7] M. B. Bolker, "Tools for general maximum likelihood estimation," R Development Core Team (2014).

[8] E. J. Gumbel, "Analysis of empirical bivariate extremal distributions," vol. 15, no. 4, pp. 414–422 (1944).

[9] M. El-Morshedy, A. H. El-Bassiouny, and A. El-Gohary, "Exponentiated inverse flexible Weibull extension distribution," *Journal of Statistics Applications and Probability*, vol. 6, no. 1, pp. 169-183 (2017).

[10] M. Nakagami, "The m-Distribution—A General Formula of Intensity Distribution of Rapid Fading," in Statistical Methods in Radio Wave Propagation, Pergamon Press Inc. (1960), doi: 10.1016/b978-0-08-009306-2.50005-4.

[11] F. R. S. de Gusmão, E. M. M. Ortega, and G. M. Cordeiro, "The generalized inverse Weibull distribution," *Statistical Papers,* vol. 52, no. 3, pp. 591–619 (2011), doi: 10.1007/s00362-009-0271-3.

[12] G. Haas, L. Bain, and C. Antle, "Inferences for the Cauchy distribution based on maximum likelihood estimators," *Biometrika,* vol. 57, no. 2, pp. 403–408 (1970), doi: 10.1093/biomet/57.2.403.

[13] A. M. Abouammoh and A. M. Alshingiti, "Reliability estimation of generalized inverted exponential distribution," *Journal of Statistical Computation and Simulation*, vol. 79, no. 11, pp. 1301-1315 (2009).

[14] R. C. Robbins and S. A. Hunt, "Analysis of Survivors More Than 10 Years After Heart Transplantation in the Cyclosporine Era: Stanford," pp. 155–164 (2004), doi: 10.1016/S1053-2498(03)00147-5.

[15] R Core Team, "R: A language and environment for statistical computing," *R Foundation for Statistical Computing* (2023). [Online]. Available: https://www.R-project.org/.

[16] A. S. Hassan, R. E. Mohamd, M. Elgarhy, and A. Fayomi, "Alpha power transformed extended exponential distribution: properties and applications," *Journal of Nonlinear Sciences and Applications*, vol. 12, no. 4, pp. 62-67 (2018).

[17] G. M. Cordeiro, E. M. M. Ortega, B. V. Popović, and R. R. Pescim, "The Lomax generator of distributions: Properties, minification process and regression model," *Applied Mathematics and Computation*, vol. 247, pp. 465–486 (2014), doi: 10.1016/j.amc.2014.09.004.

[18] G. R. Aryal, E. M. Ortega, G. G. Hamedani, and H. M. Yousof, "The Topp-Leone Generated Weibull Distribution: Regression Model, Characterizations and Applications," *International Journal of Statistics and Probability,* vol. 6, no. 1, pp. 126–141 (2016), doi: 10.5539/ijsp.v6n1p126.

[19] S. Nasiru, A. G. Abubakari, and I. D. B. Angbing, "Bounded Odd Inverse Pareto Exponential Distribution: Properties, Estimation, and Regression," *International Journal of Mathematics and Mathematical Sciences* (2021), doi: 10.1155/2021/9955657.

Received May, 2023